Chemistry & Biology 13, 825–837, August 2006 ©2006 Elsevier Ltd All rights reserved DOI 10.1016/j.chembiol.2006.06.007

Chemical Probes of UDP-Galactopyranose Mutase

Erin E. Carlson,[1] John F. May,[2] and Laura L. Kiessling[1,2,*]
[1]Department of Chemistry
[2]Department of Biochemistry
University of Wisconsin-Madison
Madison, Wisconsin 53706

Summary

Many pathogenic prokaryotes and eukaryotes possess the machinery required to assemble galactofuranose (Gal*f*)-containing glycoconjugates; these glycoconjugates can be critical for virulence or viability. Accordingly, compounds that block Gal*f* incorporation may serve as therapeutic leads or as probes of the function of Gal*f*-containing glycoconjugates. The enzyme UDP-galactopyranose mutase (UGM) is the only known generator of UDP-galactofuranose, the precursor to Gal*f* residues. We previously employed a high-throughput fluorescence polarization assay to investigate the *Klebsiella pneumoniae* UGM. We demonstrate the generality of this assay by extending it to UGM from *Mycobacterium tuberculosis*. To identify factors influencing binding, we synthesized a directed library containing a 5-arylidene-2-thioxo-4-thiazolidinone core, a structure possessing features common to ligands for both homologs. Our studies offer a blueprint for identifying inhibitors of the growing family of UGM homologs and provide insight into UGM inhibition.

Introduction

Like other hexoses, galactose can exist in the thermodynamically favored pyranose or the less favored furanose form. Galactopyranose (Gal*p*) residues are ubiquitous in the glycolipids and glycoproteins of higher and lower eukaryotes. Galactofuranose (Gal*f*) residues are less common, yet they are crucial components of the glycoconjugates in a number of pathogenic prokaryotes and both uni- and multicellular eukaryotes [1]. Often, Gal*f*-containing conjugates are necessary for viability and/or virulence. For example, Gal*f* residues have been identified in the lipopolysaccharide (LPS) O-antigen of a number of gram-negative bacteria [2–10], and the O-antigen is important in bacterial virulence [11]. There is also evidence that Gal*f* residues are essential components of the cell wall of mycobacteria such as *Mycobacterium tuberculosis*, the causative agent of tuberculosis (TB) [12–14]. Gal*f* residues have been identified in the glycoconjugates of a number of other organisms including *Salmonella* spp. [15], *Trypanosoma cruzi* (the parasite that causes Chagas disease) [16–18], and several fungi including *Aspergillus fumigatus* [19–25]. Moreover, Gal*f*-containing glycoconjugates can be highly antigenic in mammalian species because they are absent from mammals [17, 24, 26]. The distribution and biological roles of Gal*f* residues suggest that agents that block the biosynthetic incorporation of Gal*f* residues could serve as valuable biological probes or therapeutic agents [27].

UDP-galactofuranose (UDP-Gal*f*) is the biosynthetic donor of Gal*f* residues. The only enzyme known to produce this sugar-nucleotide is UDP-galactopyranose mutase (UGM or Glf). This enzyme catalyzes the isomerization of UDP-galactopyranose (UDP-Gal*p*) to UDP-Gal*f* (Figure 1A). It was first identified in prokaryotes, including several gram-negative bacteria and mycobacteria [8, 9, 28–32]. Prokaryotic UGM homologs share ~40% sequence identity; therefore, the putative genes encoding these enzymes can be readily identified [32]. Eukaryotic UGM homologs also share a high degree of identity; however, they are only distantly related to their prokaryotic counterparts [1]. Despite this challenge, strategies for identifying eukaryotic UGMs have emerged recently [1, 33]. For example, genes encoding UGM have been identified in *Leishmania major* and *Cryptococcus neoformans* [1]. Genes that encode putative UGMs have also been found in *T. cruzi*, *Aspergillus fumigatus*, and the nematode *Caenorhabditis elegans* [1, 33].

Because UGM is a critical enzyme mediating Gal*f* incorporation, we sought to identify small-molecule inhibitors. Such inhibitors could be used to probe four different issues. First, they could uncover the importance of Gal*f* residues in the relevant organisms. Gal*f* residues are found in the glycoconjugates of a number of organisms, yet the exact role that these residues play is often unknown. A second and related issue arises from the identification of genes encoding putative UGMs (*glf*s) in species not yet known to utilize Gal*f* [1]. For example, Gal*f* residues are not known to occur in *C. elegans*, but a gene has been identified (H04M03.4) that encodes a putative UGM. Genome-wide RNA interference screens suggest that downregulation of the putative UGM is deleterious [34–36]. The function of this intriguing gene product could be illuminated with inhibitors.

A third application of chemical probes of Gal*f* metabolism is to validate a specific UGM as a therapeutic target. One compelling application of UGM inhibitors is as antimycobacterial agents. Each year two to three million people die as a result of infection with *M. tuberculosis* [37]. The emergence of multidrug resistant strains of *M. tuberculosis* is a major contributor to this death toll; the need for new therapeutic agents is urgent. Several of the drugs used to treat this disease, including isoniazid, ethionamide, and ethambutol [38–41], target cell wall biosynthesis. Gal*f* is a critical constituent of an important structural component of the mycobacterial cell wall—the arabinogalactan. The arabinogalactan is crucial for mycobacterial viability, suggesting that the enzymes involved in its biosynthesis, including UGM, might serve as therapeutic targets [42]. In *M. smegmatis*, the genes encoding the enzymes that mediate Gal*f* incorporation are essential for growth [14]. This result suggests that either the Gal*f*-containing products of these enzymes are critical or that the proteins themselves fulfill a structural role within a multiprotein

*Correspondence: kiessling@chem.wisc.edu

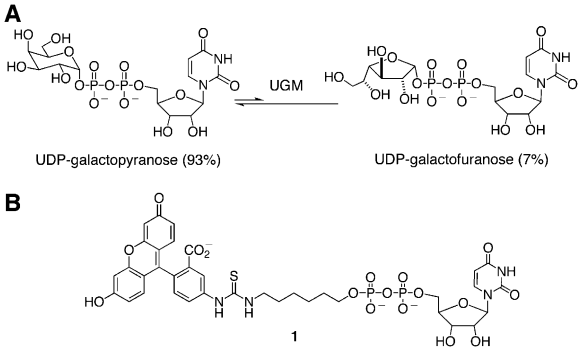

Figure 1. Nucleotide-Sugar Isomerization Reaction and Structure of Fluorescent Probe 1

(A) UGM catalyzes the isomerization of UDP-Gal*p* and UDP-Gal*f*.
(B) A fluorescent probe (1) based upon UDP was developed for fluorescence polarization assays.

complex. Chemical inhibitors provide a means to differentiate between these two possibilities; they can block UGM activity and therefore Gal*f* incorporation, but they will not prevent potentially important protein-protein interactions. Comparisons with other systems suggest that small-molecule inhibitors can complement genetic studies to illuminate the physiological role(s) or the therapeutic value of a protein target [43].

A fourth use of chemical inhibitors is to illuminate the catalytic mechanisms that underlie Gal*f* residue incorporation. Previous results from our group indicate that the UGM-mediated generation of UDP-Gal*f* occurs by a unique catalytic mechanism that involves a novel covalent flavin-galactose adduct [44]. Inhibitors could be used to elucidate further details regarding the catalytic mechanism. Additionally, they could provide insight into the architecture of the substrate binding site. The number and range of applications provide substantial incentive to identify UGM inhibitors.

Blueprints for generating inhibitors of sugar-nucleotide binding proteins, like UGM, are lacking. Although the structures of several prokaryotic UGMs have been determined by X-ray crystallography [45, 46], no structure of a substrate-enzyme complex has been reported. Some substrate-based inhibitors have been described, including sugar analogs and uridine derivatives [47–51]. However, the similarity of these to the natural substrate suggests they will inhibit enzymes that operate on related substrates. More broadly, few inhibitors of any sugar-nucleotide binding proteins have been reported; thus, we could not rely on known small-molecule scaffolds.

We reasoned that potent and selective inhibitors of UGM could be discovered from large, structurally diverse libraries of compounds. Recently, we reported the development of a fluorescence polarization-based high-throughput assay for UGM from the gram-negative bacterium, *K. pneumoniae* (UGM_{Kleb}) [52]. Using this assay, we identified several UGM ligands. Here, we evaluate the generality of this assay by testing its utility for identifying ligands of UGM from *M. tuberculosis* (UGM_{Myco}). We anticipate that the identification of ligands for UGM homologs from different organisms will afford compounds that exhibit activity against a range of prokaryotic and perhaps even eukaryotic UGMs.

We have found several compounds with activity against both UGM_{Myco} and UGM_{Kleb}. These compounds, along with those selective for a single UGM homolog, are structurally similar: they contain a five-membered heterocyclic core functionalized with a 1,3-display of substituents. To optimize the potency of these leads and to further investigate the interactions necessary for UGM-ligand binding, we synthesized a directed library based upon a 2-thioxo-4-thiazolidinone scaffold. Evaluation of the directed library provided insight into the requirements for UGM binding.

Results and Discussion

Conventional screens for enzyme inhibitors involve the assessment of catalytic activity. UGM activity is most accurately monitored by following the production of UDP-Gal*p* by high-pressure liquid chromatography (HPLC). This assay cannot be adapted readily to screen large numbers of compounds, and we envisioned that a fluorescence polarization (FP) assay could fulfill that requirement. Fluorescence polarization (FP) binding assays are readily adaptable to high-throughput screening; they require minimal sample manipulation and are highly sensitive. In FP, the emission of a fluorescent compound excited with plane-polarized light is measured. For assessing ligand binding to UGM, polarization readings depend upon whether the fluorescent probe is bound to UGM (tumbling slowly, high polarization) or free in solution (tumbling rapidly, low polarization). A compound that displaces the fluorescent probe from its binding pocket will cause the latter state. Because FP assays can detect complexes with a wide range of dissociation constants, they are proving to be especially useful for glycobiology studies. For example, FP has been applied to study lectin binding [53, 54] and to identify inhibitors of two other enzymes, MurG and *O*-GlcNAc transferase, that act on UDP-sugar substrates [55, 56].

Identifying UGM_{Kleb} Ligands

Previously, we reported using an FP assay to screen a library of 16,000 diverse small molecules designed to be cell permeable (Chembridge DIVERSet) against UGM_{Kleb} [52]. We have subsequently screened an additional 20,000 compounds (Chemical Diversity Labs, ChemDiv) against this enzyme. The compounds used in this screen were chosen to complement chemical diversity of those tested previously. These experiments, therefore, provide additional information on the types of molecular scaffolds that bind UGM.

We screened all compounds at a final concentration of 33 μM in a solution of the fluorescent probe **1** (Figure 1B) and UGM. To calibrate the FP values within each 384-well plate, we included wells containing compound **1** alone and compound **1** and UGM_{Kleb}. Data from all compounds with intrinsic fluorescence (<1%) were omitted. As a positive control, we also included a well containing UDP along with UGM and the fluorescent probe. We had shown previously that UDP is a ligand for UGM and had determined a K_d of 8.8 μM for the complex; we sought to identify compounds that interact with comparable or superior affinity. Approximately 0.4% of the compounds from both libraries were identified as hits (FP values less than or equal to those obtained for UDP).

Lead compounds were screened at a 10-fold lower concentration, and dissociation constants for the most active compounds were determined to identify the best binders (Figure 2A).

Identifying UGM_{Myco} Ligands

We sought to explore the generality and specificity of the compounds identified as UGM_{Kleb} ligands and the generality of our assay. To ascertain whether our FP assay would be useful with other UGM homologs, we tested it with the UGM from *M. tuberculosis* (UGM_{Myco}). For these studies, we needed to produce adequate quantities of UGM_{Myco}. Although it can be difficult to produce mycobacterial proteins in *E. coli*, we used a procedure similar to that employed for production of a UGM_{Kleb} [52]. We generated a construct encoding UGM_{Myco} bearing a C-terminal hexahistidine tag (His_6). To produce this tagged protein, we allowed cultures to grow overnight without induction (no isopropyl-β-D-thiogalactopyranoside); this procedure provided UGM_{Myco} in good yields (7 mg per liter of culture).

With UGM_{Myco} in hand, we sought to evaluate the generality of our high-throughput FP assay. To this end, we measured the affinity of UGM_{Myco} for fluorescent probe **1**. Given the high sequence similarity between the homologs (~40%), we anticipated that the binding affinity for UGM_{Myco} would be similar to that for UGM_{Kleb}. Indeed, the K_d value was determined to be 0.16 ± 0.005 μM for the complex of **1** and UGM_{Myco}, a value that is comparable to the K_d of the UDP fluorescein derivative (**1**)-UGM_{Kleb} complex (~0.10 μM). We also determined that UDP could competitively displace **1**. Finally, the IC_{50} value for **1** with UGM_{Myco} was determined to be 5.7 μM. These data confirm that the established FP assay could be applied to identify ligands for UGM_{Myco}.

Both commercially available libraries were screened by the aforementioned procedure. These screens afforded 55 active compounds from the ChemBridge library (0.3% hit rate) and 25 from the ChemDiv library (0.15% hit rate). As with UGM_{Kleb}, compounds active in the initial screen were tested at a 10-fold lower concentration, and the dissociation constants were determined for the best ligands (Figure 2A). Although compounds **9** and **10** were not identified as hits in the initial screens against UGM_{Kleb}, further analysis revealed that they are ligands for this enzyme (K_d values = 1.9 ± 0.2 and 1.7 ± 0.1 μM, respectively). These results highlight the utility and generality of our FP assay.

Analysis of Identified Ligands

A number of the identified compounds can bind to either enzyme homolog (compounds **6**, **9**, and **10**) (Figure 2A). Moreover, many of the identified UGM ligands share structural features (e.g., compounds **5**, **6**, **8**, **9**, **10**). These features include a five-membered thiazolidinone core that displays two carbonyl or carbonyl-like (e.g., thiocarbonyl or imino) hydrogen bond acceptors and a 1,3-arrangement of substituents on the heterocyclic core. Although other structures can serve as ligands for enzymes that act on sugar-nucleotide substrates [56], compounds with thiazolidinone cores have been identified as ligands for UDP- or TDP-sugar utilizing enzymes, including the glycosyltransferase MurG [55] and the NADPH-dependent enolpyruvyl reductase MurB [57, 58].

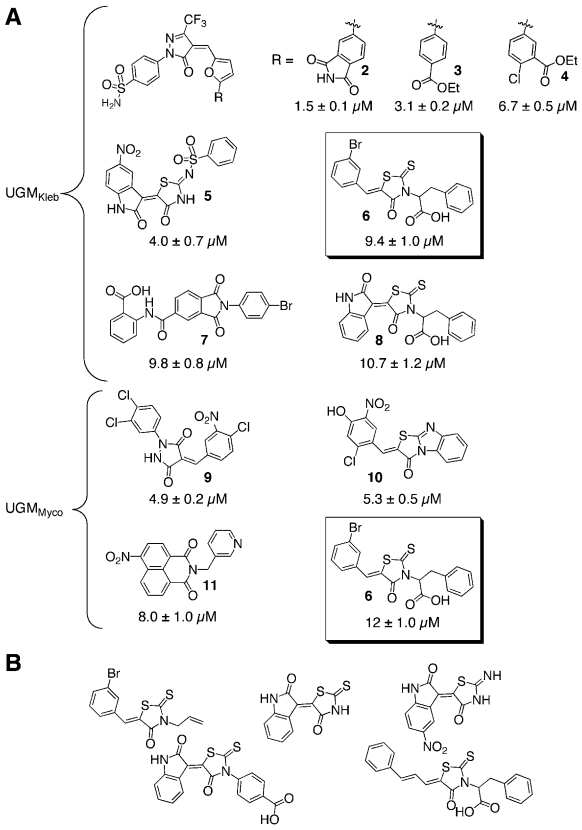

Figure 2. Compounds Identified from the High-Throughput FP Screen of Two Commercially Available Compound Libraries

(A) Ligands for UGM_{Kleb} and UGM_{Myco} are depicted. Although compounds **9** and **10** were not identified as ligands of UGM_{Kleb} in the initial screen, they were later found to have activity against this enzyme with K_d values of 1.9 ± 0.2 and 1.7 ± 0.1 μM, respectively. K_d values are reported as mean ± standard error for triplicate experiments.

(B) Examples of inactive yet structurally similar compounds present in the libraries.

Several research groups have hypothesized that these heterocycles may function as diphosphate mimics [55, 57, 59]. We speculate that they have shapes that favorably occupy the nucleotide-sugar binding site.

In addition to the common orientation of substituents on the thiazolodinone core, analysis of the active compounds revealed other common themes. Most of the substituents are aromatic groups [55, 57]. We hypothesized that one of these occupies the site of the pyrimidine base in the natural substrates. In UGM, for example, we speculate that one aromatic inhibitor substituent mimics the uracil ring in UDP-Gal*f* by engaging in π-stacking interactions with an active site tryptophan ($Trp166_{Myco}$) [45]. The UGM inhibitors identified in our screen all possess an additional aromatic group. Interestingly, a uridine-derived compound that possesses an aryl moiety linked to the 5′ position has been identified as a UGM inhibitor in a different assay (IC_{50} = 6 μM) [51]. We postulate that the second aromatic substituent interacts with the polarizable isoalloxazine ring system of the flavin cofactor [60]. The dramatic increase in binding affinity (40-fold) for fluorescein derivative **1** over UDP provides support for such a model; it suggests that UGM can

participate in extensive aromatic or hydrophobic interactions.

To further explore the binding requirements of UGM and to optimize the potency of our probes, we synthesized a directed library. We selected the thiazolidinone derivative **6** as the core scaffold because it possesses the key features of our most active compounds; it also has activity against both UGM_{Kleb} and UGM_{Myco}. An additional advantage of using this scaffold is that a solid-phase route had been described for 2-thioxo-4-thiazolidinone (or rhodanine) heterocycles [61].

To aid in the design of a directed library, we examined the structures of both the identified ligands and structurally similar but inactive compounds (Figures 2A and 2B). We first looked at which substituent varied most, with a goal of orienting the ligands in the UGM binding site. Our data indicate that the sugar binding site in UGM can accommodate a variety of groups including the structurally different Gal*p* and Gal*f* residues and the fluorescein-containing linker. We therefore reasoned that the most variable substituent would occupy this region of the substrate binding site. Because the R_2 moieties (**14**) (Figure 3) vary in both size and functional groups, we propose that this portion of the ligands occupies the sugar binding region. In contrast, little variation is tolerated at R_1. Compounds containing large or aliphatic groups at this position are inactive; therefore, we hypothesize that the R_1 group acts as a uracil or uridine mimic. This model guided the design of our directed library.

Directed Library Design, Synthesis, and Screening

The organic chemistry of thiazolidinones has a rich history [62–66]. Interest in the synthesis of compounds in this class has been driven by their biological activities. Indeed, several antidiabetic drugs contain thiazolidinone heterocycles, including rosiglitazone and pioglitazone [67]. Thiazolidinone-based compounds are also under investigation as anti-inflammatory [68, 69], antiviral [70], antibacterial [71], and anticonvulsant agents [72]. Given these activities, a number of different strategies have been developed for the formation and functionalization of the thiazolidinone heterocycles [65, 66]. As described above, we elected to synthesize a directed library based upon the 2-thioxo-4-thiazolidinone (or rhodanine) core. To facilitate the rapid assembly of compound libraries, we sought to implement a solid-phase synthetic strategy.

In 2000, Lee et al. described a solid-phase route to 2-thioxo-4-thiazolidinones [61]. This strategy yields compounds with the substitution pattern of our most active compounds; therefore, it provided a launching point for developing our synthetic route. To synthesize the core heterocycle, Lee et al. used an immobilized primary amine, such as **12**. Species of this type can readily be generated by removal of an Fmoc group from an amino acid immobilized on resin. The amine can then be exposed to thiocarbonyl diimidazole to generate the thiourea (Figure 3). Subsequent treatment with methyl thioglycolate yields the rhodanine heterocycle (**13**). We synthesized the immobilized heterocycle by using a similar protocol. We found, however, that the products synthesized with Wang resin were not as pure as those generated from 2-(4-bromomethylphenoxy)ethyl polystyrene resin.

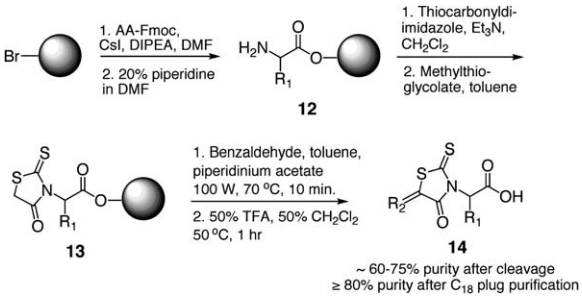

Figure 3. Synthetic Route to the Directed Library

Adaptation of the published solid-phase route to rhodanines included the development of microwave irradiation conditions to increase the efficiency of the Knoevenagel condensation.

The most problematic step in the published route is the addition of an arylalkylidene moiety, which was accomplished by a Knoevenagel condensation to afford products **14**. The desired process was effected by exposing the heterocycle to carbonyl compounds in refluxing toluene. These transformations are sluggish: the reactions of aldehydes require 12 hr and those of ketones 3 days in the presence of ammonium acetate. These conditions are inconvenient for solid-phase synthesis, so we sought alternatives.

A variety of conditions to effect Knoevenagel condensations have been reported. Often this reaction is performed at high temperatures and in the presence of a strong acid or base [66]. These conditions are not appropriate for solid-phase synthesis because they utilize strong acid, which is generally used to cleave compounds from resin, or aqueous solvent, in which most resins do not swell efficiently. Additionally, virtually all of these conditions require long reaction times and high temperatures. The problems of slow reaction kinetics are exacerbated in solid-phase synthesis, but microwave irradiation can be used to ameliorate such problems [73]. Specifically, it is well known that microwave irradiation can dramatically increase the efficiency of synthetic steps, especially those that require heat, like the desired transformations. Indeed, microwave irradiation has been used successfully to promote the Knoevenagel reaction in solution [74–76]; we reasoned it should have an even greater impact on the solid-phase reaction. To test this hypothesis, we used a model reaction between the phenylalanine derivative of intermediate **13** and *m*-bromobenzaldehyde. To optimize this process, we varied the time of irradiation, temperature, and wattage employed. With microwave irradiation (70°C, 100 watts, toluene, and piperidinium acetate), the reaction of the rhodanine heterocycle with both aldehydes and ketones proceeds to completion in only 10 min (Figure 3). These conditions are a dramatic improvement over those utilized previously, and they facilitated the assembly of the directed library.

In our focused library, we varied R_1 and R_2 to assess their roles in binding. Our pharmacophore model suggests that R_1 must be an aromatic moiety. As mentioned above, we hypothesized that this aromatic substituent interacts with a highly conserved active site tryptophan and that this interaction is critical for ligand binding. To investigate the role of this aromatic group, we generated

Table 1. Directed Library

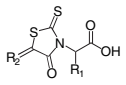

Compound	R_1	R_2	UGM_{Kleb} K_d (μM)	UGM_{Myco} K_d (μM)
15	H		>33	>33
16	CH_3		>33	>330
17			11.2	>33
18	H		>33	>330
19	CH_3		>33	>330
20			14.1	>33
21			21.3	16.0
22			6.3	6.0
23			>33	>33
24		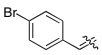	>33	9.3
25			>33	>33
26			>33	>33

Table 1. *Continued*

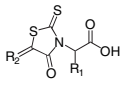

Compound	R_1	R_2	UGM_{Kleb} K_d (μM)	UGM_{Myco} K_d (μM)
27			>33	>33
28			>33	>33
29			>33	>33
30		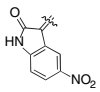	5.7	10.0
31		none	>33	>330
32	No N substitution		>330	>330

compounds **15–20**, in which the R_1 group is varied (Table 1). For comparison, these compounds contain the R_2 moieties identified in the two lead compounds (**6** and **8**).

To explore the R_2 binding site, we synthesized ten additional compounds (Table 1). Our binding model suggests that diversification of the arylalkylidene moiety will be tolerated by UGM. To evaluate the binding contributions of different R_2 moieties, we generated a series of compounds incorporating the R_1 group found in both of the lead structures but with different R_2 groups. The majority of the R_2 diversity elements included in this library was selected to explore the importance of the *m*-bromo substituent in compound **6**. We postulated that the electron-withdrawing properties of this halogen contribute to binding. Thus, we chose to synthesize *m*-chloro, *m*-iodo, *m*-fluoro-, and *m*-nitro derivatives as well as *p*- and *o*-bromo substituted compounds (**21–26**). Additionally, compounds bearing substituents with different electronic properties were also examined including *m*-methyl-, *m*-methoxy-, and unsubstituted analogs (**27–29**). Finally, a substituted isatin derivative (**30**) was synthesized to explore the binding mode of compound **8**.

These compounds were assembled by using the aforementioned synthetic route (Figure 3). Upon cleavage from the resin, the target compounds were obtained in ~60%–75% overall purity, as measured by liquid chromatography-mass spectrometry (LC-MS). The

resulting compounds were purified on a reversed phase (C_{18}) microcolumn to afford products of high purity (94% of the compounds were $\geq$80% pure, ~20%–30% yield). All compounds were obtained with a single double-bond geometry. The condensation reactions with aldehydes yielded only the Z isomer, as determined by the chemical shift of the methylene proton [77, 78]. The ketone-derived compounds were assumed to also be the thermodynamically more stable Z isomer (attempts to obtain crystals of these compounds for X-ray analysis were unsuccessful). Analysis of the library members by chiral high-performance liquid chromatography (HPLC) revealed that the configuration of the stereogenic carbon in the amino acid building blocks (Phe, Tyr, Ala) was not preserved in the products [61]. Thus, enantiomeric mixtures of all library members were assayed.

Two additional compounds, **31** and **32**, were added to the library to explore the necessity of the R_1 and R_2 substituents (Table 1). A compound lacking an R_2 substituent, **31**, was easily obtained because it is an intermediate (**13**) in the solid-phase synthetic route to compounds **14**. Compound **32**, which has no R_1 moiety, was synthesized in solution using a published protocol [79].

The resulting library, which was composed of 18 compounds, was screened in our FP assay. As described previously, each compound was dissolved in DMSO and added to a mixture of UGM_{Myco} or UGM_{Kleb} and the fluorescein probe, **1**. All compounds were tested initially at a final concentration of 330 μM, and those with activity were subsequently examined at 33 μM. From the directed library, we identified five compounds that bound to UGM_{Kleb} (**17**, **20**, **21**, **22**, **30**) and four with significant affinity for UGM_{Myco} (**21**, **22**, **24**, **30** in Table 1). Of these, three were ligands for both UGM homologs (**21**, **22**, **30**). To prepare material for further analysis, each compound that had been obtained in <94% purity during initial library generation was resynthesized and purified by HPLC. FP was then used to determine the dissociation constant of each active compound (Table 1).

The K_d value obtained for each of the active compounds is a measure of its ability to bind UGM. To assess the ability of these compounds to inhibit the catalytic activity of UGM, we employed an HPLC assay [52]. Inhibition constants (IC_{50}) were determined by monitoring UGM activity at a single substrate concentration while varying inhibitor concentration (Table 2). The data reveal that compounds with similar K_d values did not always have similar IC_{50} values. For example, compounds **6** and **8** have K_d values of approximately 10 μM (UGM_{Kleb}), but their IC_{50} values are 1.6 and 93 μM, respectively. We postulated that these differences might arise from modification of the 5-arylidene-4-thiazolidinone derivatives. We were especially interested in the reactivity of these heterocycles under conditions relevant to those in vivo because compounds of this type possess diverse and valuable biological activities.

Table 2. Selected IC_{50} Values

Compound	UGM_{Kleb} IC_{50} (μM)	UGM_{Myco} IC_{50} (μM)
5	17	—
6	1.6	65
7	4.6	—
8	93	—
9	4.0	41
10	4.0	28
21	n/d	49
22	n/d	41
24	—	35
30	n/d	>100

5-Arylidene-4-Thiazolidinone Reactivity

5-Arylidene-4-Thiazolidinones have been identified as ligands for important proteins and enzymes; several of these compounds are under investigation as therapeutic agents [55, 59, 66, 68, 69, 80–84]. Interestingly, some thiazolidinones have been shown to undergo "photochemically enhanced" binding to their targets [85, 86]. Specifically, Decicco and coworkers reported that several of the thiazolidinones they identified as tumor necrosis factor receptor-1 (TNFRc1) inhibitors displayed binding properties that depend upon light. When light is present, these compounds form covalent bonds to their protein targets. All of the compounds exhibiting this light-sensitive reactivity possess extended π systems. The general relevance of this photochemical reactivity to most thiazolidinone inhibitors is not apparent.

We focused on another potential mode of 5-arylidene-4-thiazolidinone reactivity. Inspection of the 5-arylidene-4-thiazolidinone structure suggests these compounds can serve as electrophiles. Indeed, they can undergo conjugate addition reactions with nucleophiles to afford adducts such as **33** (Figure 4) [87–90]. Still, thiazolidinones have been identified as inhibitors in cell-based screens, in which physiological nucleophiles, like the thiol glutathione, are present at high concentrations. We therefore sought to determine whether the 5-arylidene-4-thiazolidinones react under conditions relevant for their biological activity.

We tested whether two representative thiazolidinones, compounds **6** and **8**, undergo conjugate addition reactions under relevant conditions—aqueous solution at neutral pH in the presence of reducing agents (thiols). To this end, we used ultraviolet-visible spectroscopy. We reasoned that any conjugate addition process would result in a spectral change that could readily be detected. To test their reactivity, the compounds were dissolved in sodium phosphate buffer and the UV spectra obtained. As our reducing agent and thiol, we employed dithiothreitol (DTT), which was added to the compound solution at the same concentration used in assays of the catalytic activity of UGM [46]. Upon DTT treatment, a significant decrease in the absorbance of the maximum peak (380 nm for compound **6** and 425 nm for compound **8**) was observed in less than 1 min (data not shown). No additional change was observed after an hour of incubation. This decrease in absorbance intensity is indicative of the loss of an extended chromophore, and is consistent with the 1,4-conjugate addition of DTT. Additionally, analysis by LC-MS revealed the formation of a species with the expected *m/z* of adduct **33** ([M − H] expected 601.97, observed 601.9). To determine if all related rhodanine-containing compounds were reactive in our assay, we examined compounds **16**, **23**, **28**, and **29**, which possess substituents with differing electronic properties. All compounds tested underwent rapid reaction.

Our data indicate that 5-arylidene-4-thiazolidinones are reactive under physiological conditions. In addition,

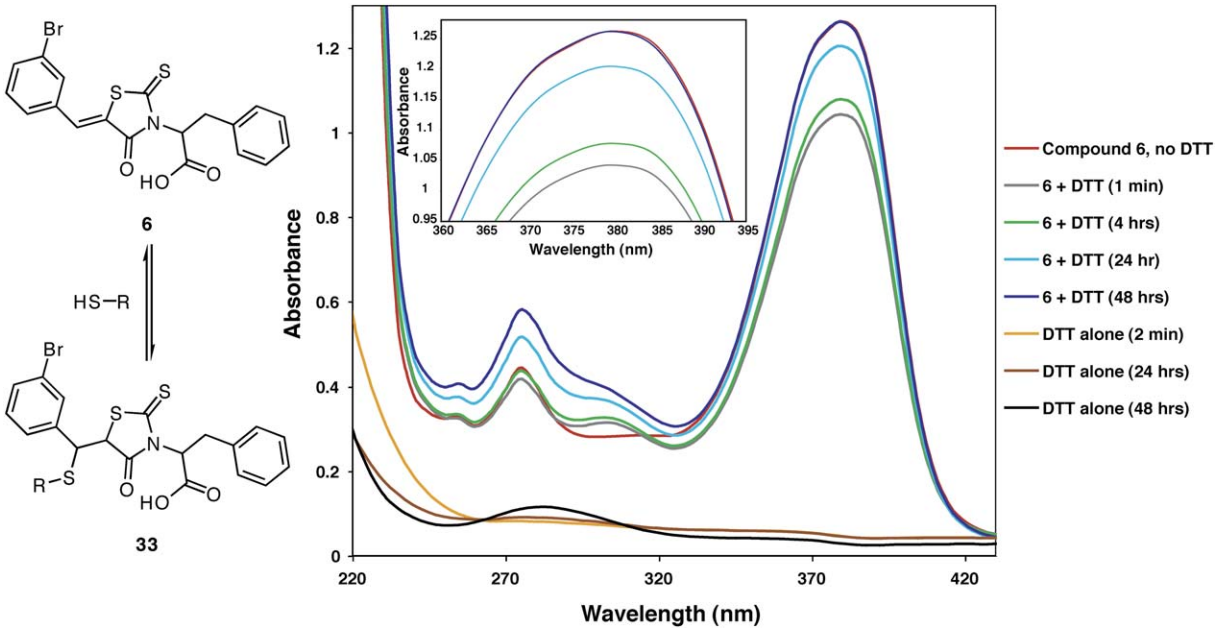

Figure 4. 5-Arylidene-4-Thiazolidinone Reactivity

Rhodanine-containing compounds (**6**) can react with thiols by 1,4-conjugate addition into the exocyclic double bond (**33**) under physiological conditions. UV-Vis spectroscopy studies show that this reaction is reversible. Examination of the UV-Vis spectra of compound **6** before and after addition of DTT is presented. Over time, DTT oxidation results in reformation of starting compound **6**. Complete restoration was seen in approximately 2 days. The increased absorbance at 290 nm is due to oxidized DTT.

they suggest that, when DTT is added to reduce UGM, adducts (e.g., **33**) form in the course of the assay. Nevertheless, the thiazolidinones inhibit UGM, and given the structure of this enzyme, we suspected that the DTT adducts (e.g., **33**) would not bind. Moreover, it seems unlikely that all of the thiazolidinone inhibitors identified in other cell-based assays function as thiol adducts. Thermal conditions in organic solvents that promote reversible conjugate addition reactions have been reported [88]; however, we sought to determine whether reversion occurs under more physiologically relevant conditions.

To test for the reversibility of thiol addition, compound **6** was mixed with DTT and allowed to react in the presence of oxygen. If the reaction is reversible, the starting compound **6** will be regenerated over time by oxidative consumption of DTT. After only 4 hr, the regeneration of thiazolidinone **6** was observed by UV-Vis spectroscopy (Figure 4). After 2 days, the starting material **6** was the only product obtained. Thus, the addition reaction of thiols to 5-arylidene-4-thiazolidinones is reversible in aqueous solutions. This result suggests that the parent compounds are the UGM inhibitors and that the observed discrepancies between the K_d and IC_{50} values are due to a decrease in the concentration of the active species in the assay. Moreover, the results indicate that differences in assay conditions might afford very different results in screens of compound collections containing 5-arylidene-4-thiazolidinone derivatives.

We performed additional experiments to probe the impact of the reversible conjugate addition reaction on our inhibition data. First, the inhibition constant of compound **24** was determined under several different conditions. Typically, the activity assay is carried out by mixing the inhibitor and the substrate in assay buffer (containing DTT); UGM is then added to initiate conversion. Under these conditions, the IC_{50} value for compound **24** is 35 μM (UGM_{Myco}). We performed experiments in which the order of addition of the various assay components was altered. In one experiment, UGM_{Myco}, **24**, and DTT were incubated in buffer for 10 min before UDP-Gal*f* was added to initiate the enzymatic reaction. A parallel experiment was performed involving a 10 min incubation of enzyme and **24** followed by simultaneous addition of DTT and UDP-Gal*f*. Exposure of the inhibitor to DTT prior to incubation with UDP-Galf gave an IC_{50} value of 50 ± 7 μM, but when no pretreatment was employed, an IC_{50} value of 39 ± 4 μM was obtained. These results also indicate that the inhibitory species is compound **24** and not its DTT adduct.

Our studies suggest that the reactivity of 5-arylidene-4-thiazolidinones complicates their use in cell-based assays or in vivo; they can react with glutathione or other free thiols within a cell. Indeed, we found that compound **6** reacts with physiologically relevant concentrations of glutathione (0.5–10 mM). Our data also indicate, however, that the compounds identified in our screen are the active species. The observed differences between our K_d and IC_{50} values likely arise from a decrease in the effective concentration of these inhibitors in the assay solution. These issues, however, do not complicate analysis of the data on UGM binding.

Features of UGM Ligands

Our original model predicted that two aromatic substituents are necessary for effective interaction with UGM. As mentioned previously, we hypothesized that R_1 acts as a uracil mimic and that it participates in aromatic-aromatic interactions. The weak affinity of the glycine and alanine-derived compounds (**15**, **16**, **18**, and **19**) for UGM is

consistent with this hypothesis. The data also suggest that, when R_1 is a phenol (**17** and **20**), the resulting compounds interact favorably with UGM_{Kleb} but not UGM_{Myco}. Thus, these enzyme homologs manifest subtle differences in their binding preferences.

The majority of the UGM ligands identified display halogen substituents at the R_2 position. Halogens can influence ligand binding interactions through different means, including van der Waals and electrostatic interactions. Interestingly, halocarbons, especially aryl and heteroaryl halides, can participate in halogen-bonding interactions (noncovalent interactions that involve halogens as electron acceptors) [91, 92]. Halogen substituents can also dramatically affect the polarizability of a ligand and thereby alter its binding properties. We anticipate that the halogen groups in the active 5-arylidene-4-thiazolidinones alter both the polarizability of the aryl moiety and the extended π system.

To probe the importance of the electronic properties of the halogen substituents, we generated **27**, which possesses a methyl group, a substituent of similar size to a bromo group but with dramatically different electronic properties. The affinity of this compound for UGM is weak. This result suggests that binding affinity depends not only on the size of the halogen substituent but also on its electronic properties.

We also examined the importance of the electronegativity of the halogen substituent by testing a series of compounds with electron-withdrawing substituents on the aryl ring. We found that compounds containing nitro (**26**) or fluoro (**23**) groups were less effective ligands than bromo derivative **6**. These results indicate that the role of the halogen substituent goes beyond its ability to act as an electron-withdrawing group. The ability of compounds bearing *m*-chloro (**21**), bromo (**6**), or iodo substituents (**22**) to bind UGM suggests that UGM is not exquisitely sensitive to the size of the halogen. The two UGM homologs, however, appear to differ in their preference for the placement of the bromo substituent. The derivative with a *p*-bromo aryl substituent (**24**) binds to UGM_{Myco} with similar affinity as the lead structure (**6**). However, UGM_{Kleb} has a weaker affinity for this analog. The *o*-bromo-containing compound (**25**) does not bind to either enzyme. This difference in affinity likely arises from steric interactions between the large *o*-bromo group and the rhodanine heterocycle, which will influence the conformation of **25**. Finally, the failure of the methoxy-substituted compound (**28**) and the unsubstituted derivative (**29**) to bind tightly to UGM is consistent with our conclusions that the electronic properties of the aryl halide influence UGM-ligand interactions.

Isatin-derived thiazolidinone derivatives are also effective ligands for UGM (compound **30** and lead structure **8**). This finding is consistent with our hypothesis that the enzyme can accommodate a range of diverse functionality at the R_2 position. Interestingly, the isatin-derived compounds display the greatest discrepancy between their K_d and IC_{50} values. When exposed to DTT, compound **8** is almost completely consumed, which suggests that its relatively poor IC_{50} values stem from its greater propensity to form the DTT adduct.

Additional support for our binding model was attained by examining the activities of compounds **31** and **32**, which represent each of the two "halves" of the lead structure. Neither the compound possessing only the R_2 (**32**) nor the R_1 (**31**) bound to UGM. Comparing the conformations of these two molecules with that of the lead compound **6** revealed no obvious conformational differences. Together, the data indicate that both portions of the lead structure are required for binding.

Modeling Substrate and Ligand Interactions with UGM

With no structural information about the substrate-UGM complex, mutagenesis and our binding data provide insight into the interactions important for binding of the sugar-nucleotide. Several amino acid side chains are thought to be critical for substrate binding in UGM_{Myco} including Trp166, Tyr161, Tyr191, Tyr328, His68, Gln165, Phe192, Asn282, Arg261, and Arg292 [46]; Trp166 and the tyrosine residues are necessary for efficient catalysis [46]. The former is thought to participate in π-stacking interactions with the uracil moiety of the substrate. Additionally, the tyrosine side chains may interact with the two sugars, ribose and galactose. Finally, several conserved arginine residues may engage in critical contacts with the substrate pyrophosphate group. These residues form a pocket near the isoalloxazine ring system of the flavin that is believed to be the active site of UGM. Docking the substrate UDP-Gal*p* into the putative active site suggests that the sugar moiety is proximal to the flavin isoalloxazine ring system (Figure 5). These results are consistent with other models of the complex [93].

Modeling studies were conducted to visualize potential binding interactions between UGM_{Myco} and active compound **6** (Figure 5). Compound **6** was manually docked into the active site; it was placed near side chains implicated in substrate binding. Examination of the resulting model reveals that the ligand **6** is similar in size to the natural substrate, UDP-Gal. Additionally, heterocycle **6** is well positioned to take advantage of many putative substrate-protein interactions, such as π stacking between the R_1 moiety and Trp166. The rhodanine moiety may participate in hydrogen bonding interactions with the protein (such as Arg261 and Arg292) in a manner similar to that of the diphosphate moiety. Finally, the R_2 substituent could interact with active site side chains (such as Tyr, His, and Phe residues) and the flavin isoalloxazine ring system. We anticipate that this model for UGM-ligand binding will aid in the future design of effective inhibitors of this enzyme.

Significance

Although Gal*f* residues are often incorporated into structures important for the viability or virulence of an organism, determining the precise function of these sugar moieties is difficult. The identification of agents to probe the enzymes involved in the biosynthesis of Gal*f*-containing glycoconjugates, including UGM, will illuminate the functions of this unique and important sugar. Using a high-throughput binding assay that is effective for several UGM homologs, including UGM_{Myco}, we identified of a number of ligands for these enzymes. Several of the identified compounds are strikingly similar in structure, containing a five-membered heterocyclic core and a 1,3-substituted display

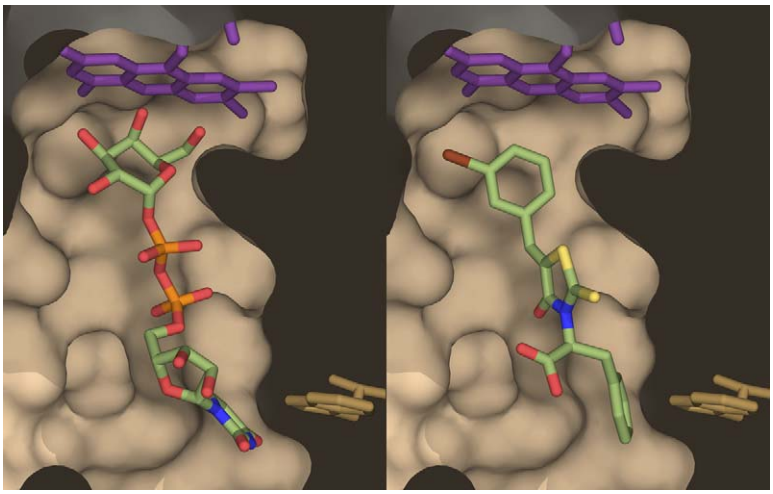

Figure 5. Models of the UGM_{Myco} Binding Site

Left, model from manual docking of the natural substrate UDP-Gal*p* into the putative active site. The substrate was placed near to amino acids thought to be critical for binding (Trp166 shown in dark yellow). This model suggests that the sugar may bind in close proximity to the isoalloxazine ring of the flavin cofactor (purple). Right, docking of lead **6** indicates that this compound is very similar in size to the natural substrate.

of aromatic substituents. The similarity of the compounds identified for both UGM_{Myco} and UGM_{Kleb} suggests that probes possessing this substituent display may interact with many or all prokaryotic UGMs; thus, compounds should emerge that can reveal the roles of galactofuranose incorporation in a number of organisms. In addition to the utility of identified ligands for study in prokaryotic organisms, we anticipate that the presented data will enable the development of probes for eukaryotic UGMs. We envision that such ligands could be used to elucidate the physiological roles of Gal*f* incorporation. Interestingly, we determined that 5-arylidene-4-thiazolidinone compounds, which have been identified as ligands of UGM and many other proteins, react with thiols under physiological conditions. Experiments to determine the efficacy of the identified compounds in a cell-based assay are ongoing and data from these experiments will illuminate the significance of the observed thiol reactivity. We also anticipate that the ligands identified here can be used to assess the validity of UGM as a potential target for antimycobacterial agents.

Experimental Procedures

Procedures for the production of UGM_{Kleb}, determination of binding constants and IC_{50} values are available in Supplemental Data, as these procedures have been published previously [44, 52].

Protein Production UGM_{Myco}

Deoxyoligonucleotide primers for polymerase chain reaction (PCR) were obtained from the University of Wisconsin Biotechnology Facility. Restriction endonucleases and polymerases were purchased from either New England Biolabs or Promega. Nickel-nitrilotriacetic acid (Ni-NTA) resin was obtained from Qiagen.

A pET-29b(+) construct containing the cloned gene encoding UGM, *glf*, from *Mycobacterium tuberculosis* was generously provided by James Naismith (University of St. Andrews) [46]. A sequence encoding a hexahistidine (His_6) tag was added at the 3′ end of the amplified gene by PCR, and the DNA was digested with DpnI (Promega, Madison, WI) and transformed into *E. coli* DH5α, giving pET29b:UGM_{Myco}-His_6. The final construct was then transformed into *E. coli* BL21(DE3) cells. Transformed cells were grown in 4 ml LB broth containing 50 μg/ml kanamycin at 37°C, and the overnight culture was used to inoculate 1 liter of terrific broth containing 50 μg/ml kanamycin, which was then incubated overnight at 37°C. Cells were harvested by centrifugation and resuspended in sodium phosphate buffer (20 mM, pH 7.4) containing 500 mM NaCl and 25 mM imidazole. Cells were disrupted via treatment with lysozyme and Triton X-100 (0.1% v/v). The resuspended cells were left on ice for 1 hr and then broken by sonication (50% duty cycle, 6 cycles of 1 min on then 2 min off, Branson 450 sonifier). Lysed cells were centrifuged at 16,000 × g for 50 min at 4°C.

The protein was purified in one of two ways: His_6-Ni-NTA agarose affinity chromatography or fast protein HisTrap HP liquid chromatography (FPLC). In the former case, the cell resuspension buffer used was 50 mM sodium phosphate (pH 8.0) containing 20 mM imidazole and 300 mM NaCl, and the supernatant fraction was applied to a Ni-NTA column (Qiagen, Valencia, CA), and the column was washed with the aforementioned resuspension buffer. To elute UGM, 50 mM sodium phosphate buffer (pH 8.0) containing 250 mM imidazole was added. The mass of purified UGM was analyzed by MALDI-TOF MS (expected *m/z*: 48,445.31; observed *m/z*: 48,435.60). In the latter case, the supernatant fraction was applied to a 1 ml HiTrap HP column (Amersham Biosciences, Piscataway, NJ), and the column was washed with the resuspension buffer. Bound protein was eluted in a linear gradient (0%–100%, 10 column volumes) to 20 mM sodium phosphate buffer (pH 7.4) containing 500 mM NaCl and 500 mM imidazole. Fractions containing purified UGM were pooled. Both methods provide an average yield of 7 mg of purified enzyme from 1 liter of culture.

Order of Addition Activity Assays

To a 50 mM sodium phosphate buffer (pH 7.0), UGM_{Myco} (12 μg) and compound were mixed. DTT was added (to 20 mM final concentration) to some samples. Samples with and without DTT were incubated 10 min at room temperature, after which DTT was added to the relevant samples to afford a final concentration of 20 mM; UDP-Gal*f* was added to a final concentration of 50 μM. The total reaction volume was 60 μl. Reactions were incubated at 37°C for 10 min, and then 60 μl of 1:1 MeOH:$CHCl_3$ solution was added to quench the reaction. The aqueous phase was analyzed for UDP-Gal*f* and UDP-Gal*p* as described in Supplemental Data.

UV-Vis Spectroscopy Reactivity Assay

Each compound was dissolved in DMSO (10 mM solution). This stock solution was added to 4 ml of a solution of 50 mM sodium phosphate buffer (pH 7) to afford a final concentration of 40–50 μM (maximum absorbance ~1). The UV-Vis spectrum of this solution was taken (Cary 50 Scan UV-Visible Spectrophotometer). Next, DTT (12.3 mg) was added (final concentration 20 mM), and the reaction was monitored at 1, 5, 30, and 60 min.

UV-Vis Spectroscopy Reversibility Assay

Compound **6** was dissolved in DMSO (10 mM solution). This stock solution was added to 4 ml of a 50 mM sodium phosphate buffer (pH 7) to afford a final concentration of 40 μM. The UV-Vis spectrum of this solution was taken (Cary 50 Scan UV-Visible Spectrophotometer). Next, 17.6 μl (11 equiv.) of a 10 mM solution of DTT was added, and the reaction was monitored at 1 min and every 5 min for the first

hour. UV spectra were also taken at 2, 4, 24, and 48 hr. A solution of DTT in sodium phosphate buffer was monitored as a control.

Docking and Modeling Studies

Each small molecule was minimized in Sybyl 7.0 Base by first computing charges with Gasteiger-Hückel. Minimization was performed by the Conjugate Gradient method (Tripos force field) terminating when the gradient energy was <0.01 kcal/mol. The minimized small molecules were exported into DeLano Scientific LLC PyMol. The small molecules were docked by manually placing the target compounds within the putative active site. Best fit was determined based upon sterics and relevant amino acid side chain interactions.

Synthesis of 32

General synthetic procedures are available as Supplemental Data. Rhodanine (300 mg, 2.52 mmol) and sodium acetate (50 mg) were dissolved in acetic acid (3.4 ml). *m*-bromobenzaldehyde (580 μl, 4.95 mmol) was added and the reaction was heated at reflux overnight. Ice was added to the reaction, and the resulting precipitant isolated by filtration (wash with cold water 2×). The orange solid was dried under reduced pressure and purified by flash chromatography (silica, 3:1 hexanes:ethyl acetate) to give 234 mg (35% yield) of a bright orange solid: ^{1}H-NMR (300 MHz, d_6-DMSO) δ 13.91 (bs, 1 H), 7.83 (t, 1 H, *J* = 1.5 Hz), 7.69 (dt, 1 H *J* = 7.8, 1.5 Hz), 7.63 (s, 1 H), 7.56 (d, 1 H, *J* = 7.8 Hz), 7.49 (t, 1 H, *J* = 7.8 Hz) ppm; ^{13}C NMR (75 MHz, d_6-DMSO) δ 195.3, 169.1, 135.3, 133.1, 133.0, 131.4, 129.7, 128.4, 127.3, 122.5 ppm; EMM (*m/z*) [M + H] calcd. for $C_{10}H_6BrNOS_2$ 298.9074, found 298.9059.

General Procedure for Solid-Phase Synthesis of the Thiazolidinones

All resin reactions were performed in fritted vessels (Biorad). An Fmoc-protected amino acid (2 equiv.) and cesium iodide (2 equiv.) were dissolved in DMF (4 ml) and added to 2-(4-bromomethylphenoxy)ethyl polystyrene resin (400 mg, 1 equiv.) that had been rinsed with DMF (3×). DIPEA (2 equiv.) was added to the resin suspension. The vessel was capped and gently agitated overnight on a tube rotator. The resin was washed with the following sequence of solvents three times: DMF (3×), THF (3×), CH_2Cl_2 (3×), acetonitrile (3×), and methanol (1×). Next, the resin was washed with DMF, and the Fmoc group was removed with a 1:4 solution of piperidine:DMF (5 ml) for 1 hr (monitored with Kaiser ninhydrin test) to give intermediate **12**. The resulting resin was again washed using the above procedure. Thiocarbonyl diimidazole (5 equiv.) and triethylamine (3 equiv.) were dissolved in CH_2Cl_2 (3 ml) and added to the resin that had been washed with CH_2Cl_2 (3×). The resulting suspension was agitated for 1 hr followed by washing with dry CH_2Cl_2 (wet solvent resulted in formation of hydrolysis products). Methyl thioglycolate (5 equiv.) was dissolved in toluene (3 ml) and immediately added to the resin. This suspension was agitated on the rotator overnight to yield the rhodanine intermediate (**13**). Formation of the heterocycle could be observed by a color change of the resin (turned pale orange/red). The resin was washed by the above described procedure and dried under high vacuum for a minimum of 5 hr. Approximately 15 mg of the resin was weighed into a microwave reaction vessel. The desired aldehyde or ketone reaction partners (4 equiv.) were dissolved in toluene (1 ml) and added to the reaction vessels. Next, piperidine (200 μl) and acetic acid (133 ml) were added resulting in solidification of the solution. Each reaction was subjected to microwave irradiation for 10 min (5 min ramp, 5 min hold) at 70°C with 100 watts of power (CEM Discovery monomodal microwave reactor, 300 W [maximum] power source). After the suspension cooled to room temperature, the resin was transferred to a fritted vessel and washed with the aforementioned sequence and dried under high vacuum.

Library members were cleaved from the resin with a trifluoroacetic acid (TFA):CH_2Cl_2 (50:50) solution (400 μl) at 50°C for 1 hr. The resin was rinsed with additional TFA and CH_2Cl_2. Solvent was removed under a stream of nitrogen to give crude products, **14**. The orange or red residue was dissolved in a minimum amount of acetonitrile (~200 μM) to which the same volume of water was added. This solution was loaded onto a reserved phase (C_{18}) plug (Alltech C_{18} extract-clean column, 200 mg). The column was washed with two volumes of water. Elution of the products was effected by addition of a 60% acetonitrile:water solution (~2 ml). The product was collected, and the solvent removed under a stream of nitrogen. Compounds were characterized by ^{1}H-NMR spectroscopy and LC-MS analysis (quantification of absorbance at 280 nm). Compounds **6**, **16**, and **17** were analyzed by chiral HPLC (*i*-PrOH with 0.1% TFA:hexanes with 0.1% TFA, 5%–55% IPA over 50 min, CHIRALCEL OD 250 × 4.6 mm column from Daicel Chemical Industries, Ltd.) and found to be racemic.

Supplemental Data

Supplemental Data include procedures for production of UGM_{Kleb} [44], procedures for the determination of binding constants and IC_{50} values [52], and general synthetic procedures. Also included are the structures of thiazolidinone-based compounds with K_d values ≤10 μM that did not show activity inhibition against UGM, a gel depicting the purification of UGM_{Myco}, and characterization data for the directed library members. These data are available at http://www.chembiol.com/cgi/content/full/13/8/825/DC1/.

Acknowledgments

We thank M. Soltero-Higgin for determining the K_d and IC_{50} values of compounds **5**, **6**, **7**, and **8** with UGM_{Kleb}, for determining the K_d value of UDP with UGM_{Kleb}, and for performing initial experiments to produce UGM_{Myco}. We also thank J. Phillips for the synthesis of compound **1** and A. Steinberg for assistance in generating Figure 5. We acknowledge N. Peters, M. Fitzgerald, and M. Hoffmann of the Keck-UWCCC Small Molecule Screening Facility for helpful discussions. MALDI-TOF MS data were obtained at the University of Wisconsin-Madison Biophysics Instrumentation Facility, which is supported by the University of Wisconsin-Madison, the National Science Foundation (BIR-9512577), and the National Institutes of Health (RR13790). This research was supported by the National Institutes of Health (AI635976). E.E.C. was supported by the National Institutes of Health Biotechnology Training Program (GM08349), and J.F.M. was supported by a National Science Foundation Graduate Research Fellowship and a Wisconsin Alumni Research Foundation Fellowship.

Received: March 16, 2006
Revised: June 5, 2006
Accepted: June 6, 2006
Published: August 25, 2006

References

1. Beverley, S.M., Owens, K.L., Showalter, M., Griffith, C.L., Doering, T.L., Jones, V.C., and McNeil, M.R. (2005). Eukaryotic UDP-galactopyranose mutase (*GLF* gene) in microbial and metazoal pathogens. Eukaryot. Cell *4*, 1147–1154.
2. Jann, B., Shashkov, A.S., Kochanowski, H., and Jann, K. (1994). Structure of the O16 polysaccharide from *Escherichia coli* O16:K1: an NMR investigation. Carbohydr. Res. *264*, 305–311.
3. Kol, O., Wieruszeski, J.M., Strecker, G., Montreuil, J., Fournet, B., Zalisz, R., and Smets, P. (1991). Structure of the O-specific polysaccharide chain from Klebsiella pneumoniae O1K2 (NCTC-5055) lipopolysaccharide. Carbohydr. Res. *217*, 117–125.
4. Dmitriev, B.A., Lvov, V.L., and Kochetkov, N.K. (1977). Complete structure of the repeating unit of the O-specific polysaccharide chain of *Shigella dysenteriae* type 3 lipopolysaccharide. Carbohydr. Res. *56*, 207–209.
5. Altman, E., Brisson, J.R., and Perry, M.B. (1988). Structure of the O-antigen polysaccharide of *Haemophilus pleuropneumoniae* serotype 3 (ATCC 27090) lipopolysaccharide. Carbohydr. Res. *179*, 245–258.
6. Perry, M.B. (1990). Structural analysis of the lipopolysaccharide of *Actinobacillus (Haemophilus) pleuropneumoniae* serotype 10. Biochem. Cell Biol. *68*, 808–810.
7. Stevenson, G., Neal, B., Liu, D., Hobbs, M., Packer, N.H., Batley, M., Redmond, J.W., Lindquist, L., and Reeves, P. (1994). Structure of the O antigen of *Escherichia coli* K-12 and the sequence for its *rfb* gene cluster. J. Bacteriol. *176*, 4144–4156.
8. Nassau, P.M., Martin, S.L., Brown, R.E., Weston, A., Monsey, D., McNeil, M., and Duncan, K. (1996). Galactofuranose

biosynthesis in *Escherichia coli* K-12: Identification and cloning of UDP-galactopyranose mutase. J. Bacteriol. *178*, 1047–1052.

9. Koplin, R., Brisson, J.-R., and Whitfield, C.J. (1997). UDP-galactofuranose precursor required for formation of the lipopolysaccharide O antigen of *Klebsiella pneumoniae* serotype 01 is synthesized by the product of the $rfbD_{KP01}$ gene. J. Biol. Chem. *272*, 4121–4128.
10. Raetz, C.R., and Whitfield, C.J. (2002). Lipopolysaccharide endotoxins. Annu. Rev. Biochem. *71*, 635–700.
11. Whitfield, C. (1995). Biosynthesis of lipopolysaccharide O antigens. Trends Microbiol. *3*, 178–185.
12. Besra, G.S., and Brennan, P.J. (1997). The mycobacterial cell envelope: a target for novel drugs against tuberculosis. J. Pharm. Pharmacol. *49*, 25–30.
13. Crick, D.C., Mahapatra, S., and Brennan, P.J. (2001). Biosynthesis of the arabinogalactan-peptidoglycan complex of *Mycobacterium tuberculosis*. Glycobiology *11*, 107R–118R.
14. Pan, F., Jackson, M., Ma, Y., and McNeil, M. (2001). Determination that cell wall galactofuran synthesis is essential for growth of mycobacteria. J. Bacteriol. *183*, 3991–3998.
15. Sarvas, M., and Nikaido, H. (1971). Biosynthesis of T1 antigen in *Salmonella*: origin of D-galactofuranose and D-ribofuranose residues. J. Bacteriol. *105*, 1063–1072.
16. De Lederkremer, R.M., and Colli, W. (1995). Galactofuranose-containing glycoconjugates in trypanosomatids. Glycobiology *5*, 547–552.
17. De Arruda, M.V., Colli, W., and Zingales, B. (1989). Terminal b-D-galactofuranosyl epitopes recognized by antibodies that inhibit *Trypanosoma cruzi* internalization into mammalian cells. Eur. J. Biochem. *182*, 413–421.
18. Previato, J.O., Gorin, P.A., Mazurek, M., Xavier, M.T., Fournet, B., Wieruszeski, J.M., and Mendoncapreviato, L. (1990). Primary structure of the oligosaccharide chain of lipopeptidophosphoglycan of epimastigote forms of *Trypanosoma cruzi*. J. Biol. Chem. *265*, 2518–2526.
19. Unkefer, C.J., and Gander, J.E. (1979). The 5-O-beta-D-galactofuranosyl-containing glycopeptide from *Penicillium charlesii*. Carbon 13 nuclear magnetic resonance studies. J. Biol. Chem. *254*, 12131–12135.
20. Parra, E., Jimenez-Barbero, J., Bernabe, M., Leal, J.A., Prieto, A., and Gomez-Miranda, B. (1994). Structural investigation of two cell-wall polysaccharides of *Penicillium expansum* strains. Carbohydr. Res. *257*, 239–248.
21. Takayanagi, T., Kimura, A., Chiba, S., and Ajisaka, K. (1994). Novel structures of N-linked high-mannose type oligosaccharides containing alpha-D-galactofuranosyl linkages in *Asperfillus niger* alpha-D-glucosidase. Carbohydr. Res. *256*, 149–158.
22. Nakajima, T., Yoshida, M., Nakamura, M., Hiura, N., and Matsuda, K. (1984). Structure of the cell wall proteogalactomannan from *Neurospora crassa*. II. Structural analysis of the polysaccharide part. J. Biochem. (Tokyo) *96*, 1013–1020.
23. Barr, K., Laine, R.A., and Lester, R.L. (1984). Carbohydrate structures of three novel phosphoinositol-containing sphingolipids from the yeast *Histoplasma capsulatum*. Biochemistry *23*, 5589–5596.
24. Levery, S.B., Toledo, M.S., Straus, A.H., and Takahashi, H.K. (1998). Structure elucidation of sphingolipids from the mycopathogen *Paracoccidioides brasiliensis*: an immunodominant beta-galactofuranose residues is carried by a novel glycosylinositold phosphorylceramide antigen. Biochemistry *37*, 8764–8775.
25. Latge, J.P.H., Kobayashi, H., Debeaupuis, J.P., Diaquin, M., Sarfati, J., Wieruszeski, J.M., Parra, E., Bouchara, J.P., and Fournet, B. (1994). Chemical and immunological characterization of the extracellular galactomannan of *Aspergillus fumigatus*. Infect. Immun. *62*, 5424–5433.
26. Golgher, D.B., Colli, W., Souto-Padron, T., and Zingales, B. (1993). Galactofuranose-containing glycoconjugates of epimastigote and trypomastigote forms of *Trypanosoma cruzi*. Mol. Biochem. Parasitol. *60*, 249–264.
27. Pederson, L.L., and Turco, S.J. (2003). Galactofuranose metabolism: a potential target for antimicrobial chemotherapy. Cell. Mol. Life Sci. *60*, 259–266.
28. Turco, S.J., and Orlandi, P.A. (1989). Structure of the phosphosaccharide-inositol core of the *Leishmania donovani* lipophosphoglycan. J. Biol. Chem. *264*, 6711–6715.
29. Pan, F., Jackson, M., Ma, Y.F., and McNeil, M. (2001). Cell wall core galactofuran synthesis is essential for growth of *Mycobacteria*. J. Bacteriol. *183*, 3991–3998.
30. Daffe, M., Brennan, P.J., and McNeil, M.R. (1990). Predominant structural features of the cell wall arabinogalactan of *Mycobacterium tuberculosis* as revealed through characterization of oligoglycosyl alditol fragments by gas chromatography/mass spectrometry and by 1H and 13C NMR analyses. J. Biol. Chem. *265*, 6734–6743.
31. Brennan, P., and Nikaido, H. (1995). The envelope of *Mycobacteria*. Annu. Rev. Biochem. *64*, 29–63.
32. Weston, A., Stern, R.J., Lee, R.E., Nassau, P.M., Monsey, D., Martin, S.L., Scherman, M.S., Besra, G.S., Duncan, K., and McNeil, M.R. (1998). Biosynthetic origin of mycobacterial cell wall galactofuranosyl residues. Tuber. Lung Dis. *78*, 123–131.
33. Bakker, H., Kleczka, B., Gerardy-Schahn, R., and Routier, F.H. (2005). Identification and partial characterization of two eukaryotic UDP-galactosepyranose mutases. Biol. Chem. *386*, 657–661.
34. Ashrafi, K., Chang, F.Y., Watts, J.L., Fraser, A.G., Kamath, R.S., Ahringer, J., and Ruvkun, G. (2003). Genome-wide RNAi analysis of *Caenorhabditis elegans* fat regulatory genes. Nature *421*, 268–272.
35. Kamath, R.S., Fraser, A.G., Dong, Y., Poulin, G., Durbin, R., Gotta, M., Kanapin, A., Le Bot, N., Moreno, S., Sohrmann, M., et al. (2003). Systematic functional analysis of the *Caenorhabditis elegans* genome using RNAi. Nature *421*, 231–237.
36. Simmer, F., Moorman, C., van der Linden, A.M., Kuijk, E., van den Berghe, P.V., Kamath, R.S., Fraser, A.G., Ahringer, J., and Plasterk, R.H. (2003). Genome-wide RNAi of *C. elegans* using the hypersensitive rrf-3 strain reveals novel gene functions. PLoS Biol. *1*, E12.
37. World Health Organization (2002). Tuberculosis. In Fact Sheet Number 104 (Geneva: World Health Organization).
38. Barry, C.E. (1997). New horizons in the treatment of tuberculosis. Biochem. Pharmacol. *54*, 1165–1172.
39. Takayama, K., and Kilburn, J.O. (1989). Inhibition of synthesis of arabinogalactan by ethambutol in *Mycobacterium smegmatis*. Antimicrob. Agents Chemother. *33*, 1493–1499.
40. Quemard, A., Lacave, C., and Laneelle, G. (1991). Isoniazid inhibition of mycolic acid synthesis by cell extracts of sensitive and resistant strains of *Mycobacterium aurum*. Antimicrob. Agents Chemother. *35*, 1035–1039.
41. Ramaswamy, S., and Musser, J.M. (1998). Molecular genetic basis of antimicrobial agent resistance in *Mycobacterium tuberculosis*: 1998 update. Tuber. Lung Dis. *79*, 3–29.
42. Brennan, P.J. (2003). Structure, function, and biogenesis of the cell wall of *Mycobacterium tuberculosis*. Tuberculosis (Edinb.) *83*, 91–97.
43. Bishop, A.C., Ubersax, J.A., Petsch, D.T., Matheos, D.P., Gray, N.S., Blethrow, J., Shimizu, E., Tsein, J.Z., Schultz, P.G., Rose, M.D., et al. (2000). A chemical switch for inhibitor-sensitive alleles of any protein kinase. Nature *407*, 395–401.
44. Soltero-Higgin, M., Carlson, E.E., Gruber, T.D., and Kiessling, L.L. (2004). A unique catalytic mechanism for UDP-galactopyranose mutase. Nat. Struct. Mol. Biol. *11*, 539–543.
45. Sanders, D.A.R., Staines, A.G., McMahon, S.A., McNeil, M.R., Whitfield, C.J., and Naismith, J.H. (2001). UDP-galactopyranose mutase has a novel structure and mechanism. Nat. Struct. Biol. *8*, 858–863.
46. Beis, K., Srikannathasan, V., Liu, H., Fullerton, W.B.F., Bamford, V.A., Sanders, D.A.R., Whitfield, C., McNeil, M.R., and Naismith, J.H. (2005). Crystal structures of *Mycobacteria tuberculosis* and *Klebsiella pneumoniae* UDP-galactopyranose mutase in the oxidised state and *Klebsiella pneumoniae* UDP-galactopyranose mutase in the (active) reduced state. J. Mol. Biol. *348*, 971–982.
47. Caravano, A., Mengin-Lecreulx, D., Brandello, J.-M., Vincent, S.P., and Sinay, P. (2003). Synthesis and inhibition properties of conformational probes for the mutase-catalyzed UDP-galactopyranose/furanose interconversion. Chemistry *9*, 5888–5898.

48. Lee, R.E., Smith, M.D., Nash, R.J., Griffiths, R.C., McNeil, M., Grewel, R.K., Yan, W., Besra, G.S., Brennan, P., and Fleet, G.W.J. (1997). Inhibition of UDP-Gal mutase and mycobacterial galactan biosynthesis by pyrrolidine analogues of galactofuranose. Tetrahedron Lett. *38*, 6733–6736.
49. Ghavami, A., Chen, J.J., and Pinto, B.M. (2004). Synthesis of a novel class of sulfonium ions as potential inhibitors of UDP-galactopyranose mutase. Carbohydr. Res. *339*, 401–407.
50. Veerapen, N., Yuan, Y., Sanders, D.A.R., and Pinto, B.M. (2004). Synthesis of novel ammonium and selenonium ions and their evaluation as inhibitors of UDP-galactopyranose mutase. Carbohydr. Res. *339*, 2205–2217.
51. Scherman, M.S., Winans, K.A., Stern, R.J., Jones, V., Bertozzi, C.R., and McNeil, M.R. (2003). Drug targeting Mycobacterium tuberculosis cell wall synthesis: development of a microtiter plate-based screen for UDP-galactopyranose mutase and identification of an inhibitor from a uridine-based library. Antimicrob. Agents Chemother. *47*, 378–382.
52. Soltero-Higgin, M., Carlson, E.E., Phillips, J.H., and Kiessling, L.L. (2004). Identification of inhibitors for UDP-galactopyranose mutase. J. Am. Chem. Soc. *126*, 10532–10533.
53. Weatherman, R.V., Mortell, K.H., Chervenek, M., Kiessling, L.L., and Toone, E.J. (1996). Specificity of C-glycoside complexation by mannose/glucose specific lectins. Biochemistry *35*, 3619–3624.
54. Weatherman, R.V., and Kiessling, L.L. (1996). Fluorescence anisotropy assays reveal affinities of *C*- and *O*-glycosides for concanavalin A. J. Org. Chem. *61*, 534–538.
55. Helm, J.S., Hu, Y.N., Chen, L., Gross, B., and Walker, S. (2003). Identification of active-site inhibitors of MurG using a generalizable, high-throughput glycosyltransferase screen. J. Am. Chem. Soc. *125*, 11168–11169.
56. Gross, B.J., Kraybill, B.C., and Walker, S. (2005). Discovery of *O*-GlcNAc transferase inhibitors. J. Am. Chem. Soc. *127*, 14588–14589.
57. Andres, C.J., Bronson, J.J., D'Andrea, S.V., Deshpande, M.S., Falk, P.J., Grant-Young, K.A., Harte, W.E., Ho, H.T., Misco, P.F., Robertson, J.G., et al. (2000). 4-thiazolidinones: novel inhibitors of the bacterial enzyme MurB. Bioorg. Med. Chem. Lett. *10*, 715–717.
58. Bronson, J.J., DenBleyker, K.L., Falk, P.J., Mate, R.A., Ho, H.-T., Pucci, M.J., and Snyder, L.B. (2003). Discovery of the first antibacterial small molecule inhibitors of MurB. Bioorg. Med. Chem. Lett. *13*, 873–875.
59. Sim, M.M., Ng, S.B., Buss, A.D., Crasta, S.C., Goh, K.L., and Lee, S.K. (2002). Benzylidene rhodanines as novel inhibitors of UDP-N-acetylmuramate/L-alanine ligase. Bioorg. Med. Chem. Lett. *12*, 697–699.
60. Meyer, E.A., Castellano, R.K., and Diederich, F. (2003). Interactions with aromatic rings in chemical and biological recognition. Angew. Chem. Int. Ed. Engl. *42*, 1210–1250.
61. Lee, C.L., and Sim, M.M. (2000). Solid-phase combinatorial synthesis of 5-arylalkylidene rhodanine. Tetrahedron Lett. *41*, 5729–5732.
62. Augustin, M., and Rudolf, W.-D. (1974). Substituted rhodanines. J. Prakt. Chem. *316*, 520–524.
63. Mallick, S.K., and Martin, A.R. (1971). Synthesis and antimicrobial evaluation of some 5-(5-nitrofurylidene)rhodanines, 5-(5-nitrofurylidene)thiazolidine-2,4-diones, and their vinylogs. J. Med. Chem. *14*, 528–532.
64. Sing, W.T., Lee, C.L., Yeo, S.L., Lim, S.P., and Sim, M.M. (2001). Arylalkylidene rhodanine with bulky and hydrophobic functional group as selective HCVNS3 protease inhibitor. Bioorg. Med. Chem. Lett. *11*, 91–94.
65. Singh, S.P., Parmar, S.S., Raman, K., and Stenberg, V.I. (1981). Chemical and biological activity of thiazolidinones. Chem. Rev. *81*, 175–203.
66. Lesyk, R.B., and Zimenkovsky, B.S. (2004). 4-Thiazolidones: centenarian history, current status and perspectives for modern organic and medicinal chemistry. Curr. Org. Chem. *8*, 1547–1577.
67. Day, C. (1999). Thiazolidinediones: a new class of antidiabetic drugs. Diabet. Med. *16*, 179–192.
68. Seno, K., Okuno, T., Nishi, K., Murakami, Y., Watanabe, F., Matsuura, T., Wada, M., Fujii, Y., Yamada, M., Ogawa, T., et al. (2000). Pyrrolidine inhibitors of human cytosolic phospholipase A(2). J. Med. Chem. *43*, 1041–1044.
69. Wiesenberg, I., Chiesi, M., Missbach, M., Spanka, C., Pignat, W., and Carlberg, C. (1998). Specific activation of the nuclear receptors PPARgamma and RORA by the antidiabetic thiazolidinedione BRL 49653 and the antiarthritic thiazolidinedione derivative CGP 52608. Mol. Pharmacol. *53*, 1131–1138.
70. Sudo, K., Matsumoto, Y., Matsushima, M., Fujiwara, M., Konno, K., Shimotohno, K., Shigeta, S., and Yokota, T. (1997). Novel hepatitis C virus protease inhibitors: thiazolidine derivatives. Biochem. Biophys. Res. Commun. *238*, 643–647.
71. Foye, W.O., and Tovivich, P. (1977). N-Glucopyranosyl-5-aralkyidenerhodanines: synthesis and antibacterial and anti-viral activities. J. Pharm. Sci. *66*, 1607–1611.
72. Mishra, S., Srivastava, S.K., and Srivastava, S.D. (1997). Synthesis of 5-arylidene-2-aryl-3-(phenothiazino/benzotriazoloacetamidyl)-1,3-thiazolidine-4-ones as antiinflammatory, anticonvulsant, analgesic and antimicrobial agents. Indian J. Chem. Sect. B *36*, 826–830.
73. Blackwell, H.E. (2003). Out of the oil bath and into the oven—microwave-assisted combinatorial chemistry heats up. Org. Biomol. Chem. *1*, 1251–1255.
74. de la Cruz, P., Diez-Barra, E., Loupy, A., and Langa, F. (1996). Silica gel catalysed Knoevenagel condensation in dry media under microwave irradiation. Tetrahedron Lett. *37*, 1113–1116.
75. Lacova, M., Gasparova, R., Loos, D., Liptay, T., and Pronayova, N. (2000). Effect of microwave irradiation on the condensation of 6-substituted 3-formylchromones with some five-membered heterocyclic compounds. Mol. *5*, 167–178.
76. Yang, D.-H., Chen, Z.-C., Chen, S.-Y., and Zheng, Q.-G. (2003). A convenient synthesis of 5-benzylidenethiazolidine-2, 4-diones under microwave irradiation without solvent. J. Chem. Res. *2003*, 330–331.
77. Ohishi, Y., Mukai, T., Nagahara, M., Yajima, M., Kajikawa, N., Miyahara, K., and Takano, T. (1990). Preparations of 5-alkylmethylidene-3-carboxymethylrhodanine derivatives and their aldose reductase inhibitory activity. Chem. Pharm. Bull. (Tokyo) *38*, 1911–1919.
78. Momose, Y., Meguro, K., Ikeda, H., Hatanaka, C., Oi, S., and Sohda, T. (1991). Studies on antidiabetic agents. X. Synthesis and biological activities of pioglitazone and related compounds. Chem. Pharm. Bull. (Tokyo) *39*, 1440–1445.
79. Khodair, A.J. (2002). A convenient synthesis of 2-arylidene-5*H*-thiazolo[2,3-b]quinazoline-3,5[2*H*]-diones and their benzoquinazoline derivatives. J. Heterocycl. Chem. *39*, 1153–1160.
80. Maccari, R., Ottana, R., Curinga, C., Vigorita, M.G., Rakowitz, D., Steindl, T., and Langer, T. (2005). Structure-activity relationships and molecular modelling of 5-arylidene-2,4-thiazolidinediones active as aldose reductase inhibitors. Bioorg. Med. Chem. *13*, 2809–2823.
81. Orchard, M.G., Neuss, J.C., Galley, C.M.S., Carr, A., Porter, D.W., Smith, P., Scopes, D.I.C., Haydon, D., Vousden, K., Stubberfield, C.R., et al. (2004). Rhodanine-3-acetic acid derivatives as inhibitors of fungal protein mannosyl transferase 1 (PMT1). Bioorg. Med. Chem. Lett. *14*, 3975–3978.
82. Bruno, G., Costantino, L., Curinga, C., Maccari, R., Monforte, F., Nicolo, F., Ottana, R., and Vigorita, M.G. (2002). Synthesis and aldose reductase inhibitory activity of 5-arylidene-2,4-thiazolidinediones. Bioorg. Med. Chem. *10*, 1077–1084.
83. Heerding, D.A., Christmann, L.T., Clark, T.J., Holmes, D.J., Rittenhouse, S.F., Takata, D.T., and Venslavsky, J.W. (2003). New benzylidenethiazolidinediones as antibacterial agents. Bioorg. Med. Chem. Lett. *13*, 3771–3773.
84. Cutshall, N.S., O'Day, C., and Prezhdo, M. (2005). Rhodanine derivatives as inhibitors of JSP-1. Bioorg. Med. Chem. Lett. *15*, 3374–3379.
85. Carter, P.H., Scherle, P.A., Muckelbauer, J.K., Voss, M.E., Liu, R.-Q., Thompson, L.A., Tebben, A.J., Solomon, K.A., Lo, Y.C., Li, Z., et al. (2001). Photochemically enhanced binding of small molecules to the tumor necrosis factor receptor-1 inhibits the binding of TNF-α. Proc. Natl. Acad. Sci. USA *98*, 11879–11884.

86. Voss, M.E., Carter, P.H., Tebben, A.J., Scherle, P.A., Brown, G.D., Thompson, L.A., Xu, M., Lo, Y.C., Yang, G., Liu, R.-Q., et al. (2003). Both 5-arylidene-2-thioxodihydropyrimidine-4,6(1*H*,5*H*)-diones and 3-thioxo-2,3-dihydro-1*H*-imidazo[1,5-*a*]indol-1-ones are light-dependent tumor necrosis factor-α antagonists. Bioorg. Med. Chem. Lett. *13*, 533–538.
87. Bowden, K., and Chana, R.S. (1990). Structure-activity relations. Part 6. The alkaline hydrolysis of 3-methyl-5-methylidene- and 3,5-dimethylthiaxolidine-2,4-diones. The addition of thiols of 3-methyl-5-methylidenethiazolidine-2,4-dione. J. Chem. Soc., Perkin Trans. 2 *12*, 2163–2166.
88. Mustafa, A., Asker, W., and Sobhy, M.E.E. (1960). On the reactivity of exocyclic double bond in 5-arylidene-3-aryl-2,4-thiazolidediones; their reaction with diazoalkanes, *p*-thiocresol and piperidine. J. Am. Chem. Soc. *82*, 2597–2601.
89. Yadav, L.D.S., Dubey, S., and Singh, S.P. (2002). A convenient synthesis of 3,5-diarylthieto[2,3-*d*]thiazole-2-thiones, and expansion of their thiete ring with carbon disulphide. Indian J. Chem. *41*, 1234–1237.
90. Nagase, H. (1974). Studies on fungicides. 24. Reaction of 5-methyoxycarbonyl-methylidene-2-thioxo(or oxo)-4-thiazolidones with ortho-aminobenzenethiol and other thiols. Chem. Pharm. Bull. (Tokyo) *22*, 42–49.
91. Metrangolo, P., Neukirch, H., Pilati, T., and Resnati, G. (2005). Halogen bonding based recognition processes: a world parallel to hydrogen bonding. Acc. Chem. Res. *38*, 386–395.
92. Auffinger, P., Hays, F.A., Westhof, E., and Ho, P.S. (2004). Halogen bonds in biological molecules. Proc. Natl. Acad. Sci. USA *101*, 16789–16794.
93. Yuan, Y., Wen, X., Sanders, D.A.R., and Pinto, B.M. (2005). Exploring the mechanism of binding of UDP-galactopyranose to UDP-Galactopyranose Mutase by STD-NMR spectroscopy and molecular modeling. Biochemistry *44*, 14080–14089.